JOURNAL OF MATERIALS SCIENCE 16 (1981) 1935–1944

Calculation of cooling and heating rates and transformation curves for the preparation of metallic glasses

H. -W. BERGMANN, H. U. FRITSCH, G. HUNGER
Institut für Werkstoffkunde und Werkstofftechnik, Technische Universität Clausthal, Agricolastrasse 2, D-3392 Clausthal-Zellerfeld, West Germany

A Fortran program is described for calculating and plotting time–temperature–crystallization curves during rapid heating and cooling by, for example, laser glazing, electron beam melting, melt-spinning or other techniques for the production of metallic glasses and metastable phases. Experiments were carried out to demonstrate the applicability of the program. In the case of Fe–B alloys produced by melt-spinning the behaviour during continuous cooling and isothermal annealing could be predicted. In the case of Ni–Nb alloys the program was used to establish the experimental conditions for the formation of metallic glass by electron beam melting. The program was also used to determine the conditions necessary for glass formation by laser melting a surface layer of boron alloyed to the surface of an Fe–Cr substrate.

1. Introduction

Metallic glasses are at the present time of universal interest as they exhibit many new and fascinating properties [1–5]. There are several ways of preparing metallic glasses [3–7]. Unfortunately it is not possible owing to the high cooling rate required in such techniques to measure many of the relevant production parameters.

Several years ago, Ruhl [8] attempted to calculate the cooling curves. These calculations dealt with the conditions pertaining to melt-spinning or splat cooling. Anthony and Cline [9, 10] subsequently determined the heating and cooling curves for the retention or formation of metallic glass layers on massive specimens by laser or electron beam glazing. The question of whether a thin layer is crystalline or glassy for a particular cooling rate can be answered using the corresponding time–temperature–transformation (TTT) curves developed by Davies or Uhlmann and co-workers [11, 12]. As shown by Grange and Kiefer [13] the isothermal TTT curves can be modified to obtain continuous cooling (CT) curves.

In the present work a Fortran program is presented which predicts the heating, cooling and crystallization behaviour of metallic glasses. The use of the program is demonstrated in three applications.

2. Mathematical considerations

In a homogeneous, isotropic material the non-stationary heat flow can be described by the partial differential equation

$$\frac{\partial T}{\partial t} = \frac{\lambda}{C_p \cdot \rho} \frac{\partial^2 T}{\partial x^2} \quad (1)$$

where T is the temperature, t is the time and x is the distance from the surface. The heat conductivity λ, the specific heat C_p as well as the density ρ are temperature dependent material parameters, and must be changed if a phase transformation occurs. On the other hand, the temperature dependence of these parameters is relatively weak and the average value over the temperature range considered could be taken. The errors introduced must be examined in each case. If too great, Equation 1 can be solved separately for each phase and a continuous transition between phases imposed. In this work, Equation 1 was considered as a difference equation and instead of an analytical solution the numerical approximation suggested

0022–2461/81/071935–10$03.00/0

by Schmidt [14] was adopted which led to

$$T_{n,k+1} = \tfrac{1}{2}(T_{n+1,k} + T_{n-1,k}). \quad (2)$$

The subscript k signifies the kth temperature step Δt ($t = k \cdot \Delta t$) and the subscript n is the nth interval Δx, ($x = n \cdot \Delta x$).

If one considers a body without heat sources or sinks, the cooling profile can be described by Equation 2 if heat conduction takes place in the cooling material. This is the case for example in the cooling of a molten layer on the surface of a massive specimen (e.g. laser glazing or electron beam glazing). If no or limited heat transfer to the cooling material takes place, as for example between melt and wheel in the melt-spinning process, the heat transfer coefficient must be known. (In the case of melt-spinning, the fact that the heat transfer coefficient changes abruptly if the ribbon leaves the wheel must be taken into account.)

If the temperature at the surface of a specimen is to be calculated in the first interval and if the variation of the surface temperature with time is not known but only the surrounding temperature is known, then an intermediate point with a distance from the surface $s = \lambda/\alpha$ and ordinate T_{surr} must be constructed to calculate the surface conditions

$$-\lambda \frac{dT}{dx} = \alpha(T - T_{surr}). \quad (3)$$

Thus the temperature variation over the surface at each point in time can be calculated.

The treatment of internal heat sources or sinks, e.g. latent heats of phase transformations, have not been considered previously but can be taken into account and will be discussed later. If heating curves are required e.g. laser melting or electron beam melting, then external heat sources must be considered. This can only be done using Equation 2 in which between the nth and $(n+1)$th time interval ($n = 0, 1, 2 \ldots$) an increase in temperature corresponding to the beamed energy is imposed on the surface. Thus the temperature increase at the surface is combined with heat transfer into the body of the material.

Since melting and nucleation phenomena are to be described it is absolutely necessary to consider the various phases which can arise. On heating for example at the melting point the temperature will not increase until the latent heat of melting has been supplied. Thereafter the temperature continues to increase. If the boiling point is attained, the temperature again remains constant until the heat evaporation has been absorbed. Evaporation then causes a displacement of the surface and thus of the origin.

On solidification the problem is more difficult as it is necessary to differentiate between the glassy and the crystalline states. The TT crystallization curves are calculated using the expression derived by Davies [11], which describes the proportion, z, of crystallized material as a function of t (e.g. $z = 10^{-6} \equiv$ nucleation, $z = 10^{0} \equiv$ complete crystallization). The parameters in Equation 4 are available in the literature or can be measured.

$$t = \frac{9.3}{kT}\eta(T) \times \left\{ \frac{z \cdot a_0^2 \exp\left(\dfrac{1.024}{T_r^3 \cdot \Delta T_r^2}\right)}{f^3 N_v^0 \left[1 - \exp\left(-\Delta H_f^m \cdot \dfrac{\Delta T_r}{RT}\right)\right]^3} \right\}^{1/4} \quad (4)$$

where $\eta(T)$ is the viscosity, z is the volume fraction crystallized, a_0 is the mean atomic diameter, N_v^0 is the number of atoms per unit cell, $T_r = T/T_m$, T_m is the melting point, $\Delta T_r = (T_m - T)/T_m$, ΔH_f^m is the molar heat of fusion and f is the fraction of sites on the crystal surface at which growth is possible e.g. $f = 1$ for rough surfaces, $f = 0.2\Delta T_r$ for smooth surfaces.

These TTT curves were calculated for isothermal annealing and transformed into CT curves. Fig. 1 shows some typical curves of both types. If a cooling curve intersects a CT curve for z vol% (e.g. $z = 10^{-6}$, $z = 10^{-1}$ etc.) then the corresponding amount of latent heat is released. If cooling is sufficiently rapid to avoid intersecting the curves, then below the glass transition temperature, T_g, it is assumed that heat is released on cooling corresponding to the value of the specific heat at each temperature.

In the case of melt-spinning, crystallization is normally best described using homogeneous nucleation. For laser glazing or electron beam glazing, however, heterogeneous nucleation cannot be neglected because at the melt–substrate interface no new nucleation of crystals is necessary. The movement, s, of the liquid–solid interface into the liquid is then controlled by the crystal growth rate u_c and hence given by

$$s = \int u_c(T)\, dt \quad (5)$$

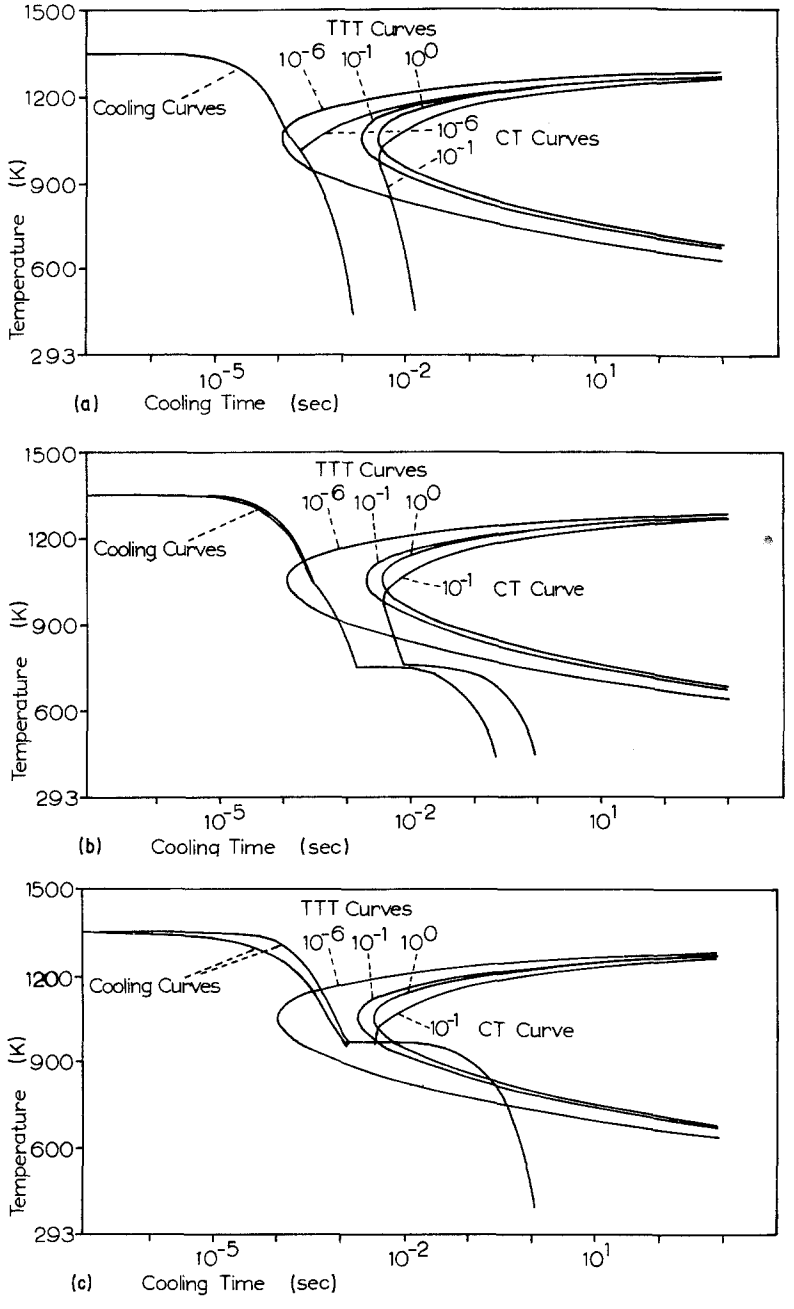

Figure 1 Calculated solidification during melt-spinning of $Fe_{83}B_{17}$ tapes with different thicknesses: (a) 10 μm, (b) 20 μm and (c) 50 μm. Cooling curves and TTT curves as well as CT curves are shown for different volume fractions z of crystallized material ($z = 10^{-6}$, 10^{-1}, 10^{0}). At the moment of separation from the wheel (at an assumed angle of 60°) the tapes have been quenched down to different temperatures in the three diagrams. Upper and lower cooling curves correspond to the top-side and contact-side of the tape.

with

$$u_c = \frac{f \cdot k \cdot T}{3\pi \cdot a_0^2 \eta(T)} \left[1 - \exp\left(-\Delta H_f^m \frac{\Delta T_r}{RT}\right)\right] \quad (6)$$

as suggested by Uhlmann [12]. Then

$$s = \sum_n s_n = \sum_n \Delta t_n \frac{f \cdot k \cdot T_n}{3\pi a_0^2 \eta(T_n)} \times \left[1 - \exp\left(-\Delta H_f^m \frac{\Delta T_r}{RT}\right)\right]. \quad (7)$$

If the cooling rate is sufficiently high so that only part of the melt crystallizes onto the surface of the substrate, then in the remaining undercooled liquid, crystallization can be described in terms of homogeneous nucleation.

3. Description of the Fortran program

The Fortran program consists of three subprograms, one each for heating, cooling and crystallization. The three subprograms can be incorporated into the operative program according to the particular

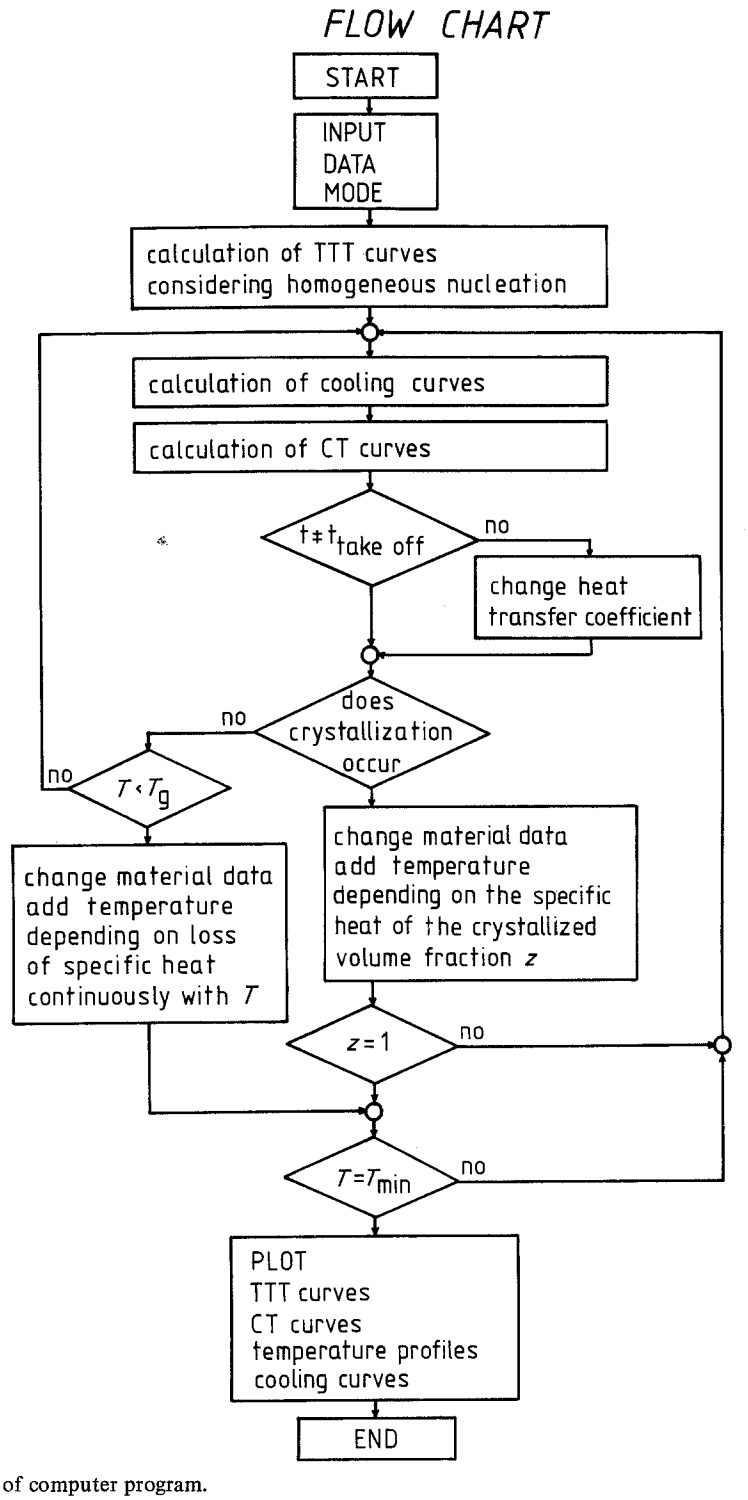

Figure 2 Flow chart of computer program.

problem being considered. The program consists of 800 cards and requires 50 K storage and 200 K background storage (TR440 computer). The time required depends on the resolution required. For the examples cited the time was of the order of 1000 sec. Fig. 2 shows a flow diagram of the program. Using the input data listed in Table I the time dependent temperature contours can be calculated. First order transformations are taken into account. The numerical predictions of the

program could be verified by direct measurement of the macroscopic specimen.

4. Applications

4.1. Melt-spinning

$Fe_{83}B_{17}$ was prepared from powder and converted by melt-spinning under vacuum into glassy ribbons between 10 and 60 μm thick. The wheel diameter was 120 mm and speeds up to 6000 rpm were used depending on the thickness required. The ribbon leaves the wheel between 45 and 60°. The as-quenched tapes were chemically analysed (Fe = 83.4 at %, B = 16.6 at %) and were examined by X-ray analysis and electron microscopy. The 10 μm bands exhibited isolated regions of dendritic solidification in an otherwise amorphous matrix. The 60 μm ribbons were completely crystalline [15].

TABLE I Input data for $Fe_{83}B_{17}$

Parameter	Value
Thermal conductivity	0.303 J cm^{-1} sec^{-1} K^{-1}
Density	6.93 g cm^{-1}
Specific heat	0.503 J g^{-1} K^{-1}
Heat transfer coefficients	
melt/wheel	80000 W m^{-1} K^{-1}
melt/air	40 W m^{-1} K^{-1}
Temperature of surroundings	293 K
Temperature of melt	1500 K
Undercooling of the melt in the melt puddle	*ca* 100 K
Solidification temperature	1448 K
Molecular weight	48.1 gmol
Atomic diameter	2.8 × 10^{-10} m
Number of atoms per unit cell	2
Molar heat of fusion	13760 J mol^{-1}
Viscosity = K exp ($E/2T$)	
K	9.8 × 10^{-11} poise
E	50 070 kcal mole^{-1}
Thickness of ribbon	10, 20, 50 μm

Fig. 1 shows calculated cooling curves for

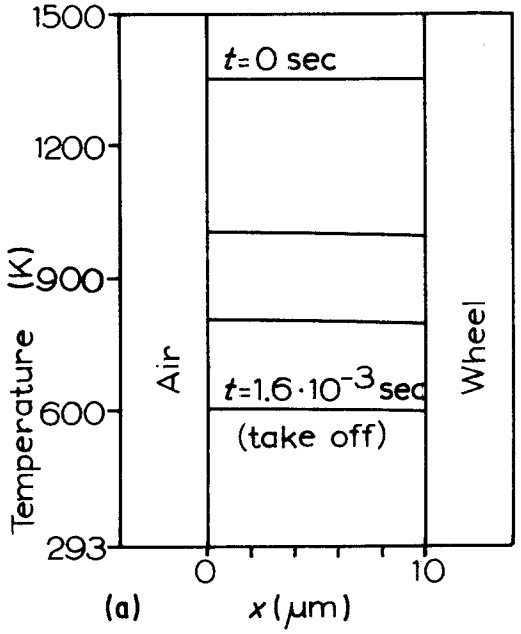

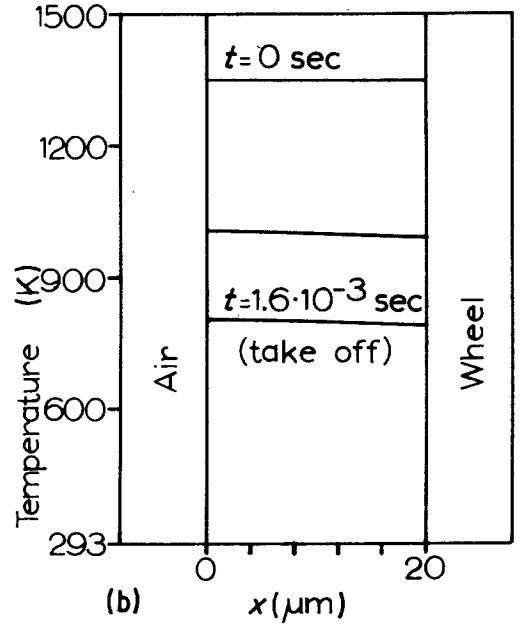

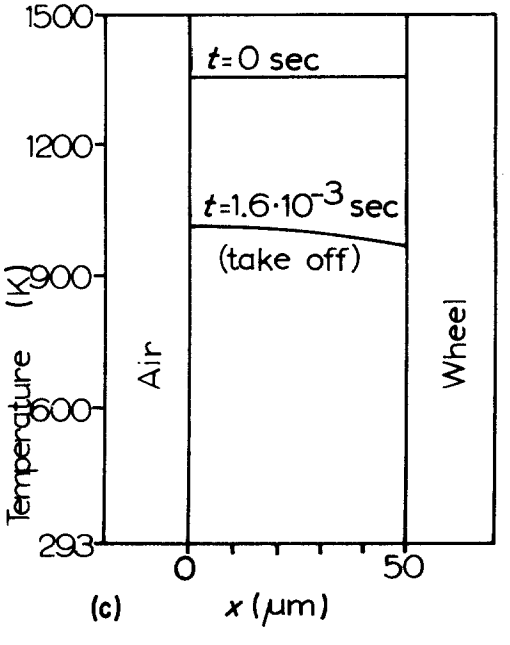

Figure 3 The through thickness temperature profiles which are related to Fig. 1 are shown: (a) 10 μm, (b) 20 μm and (c) 50 μm.

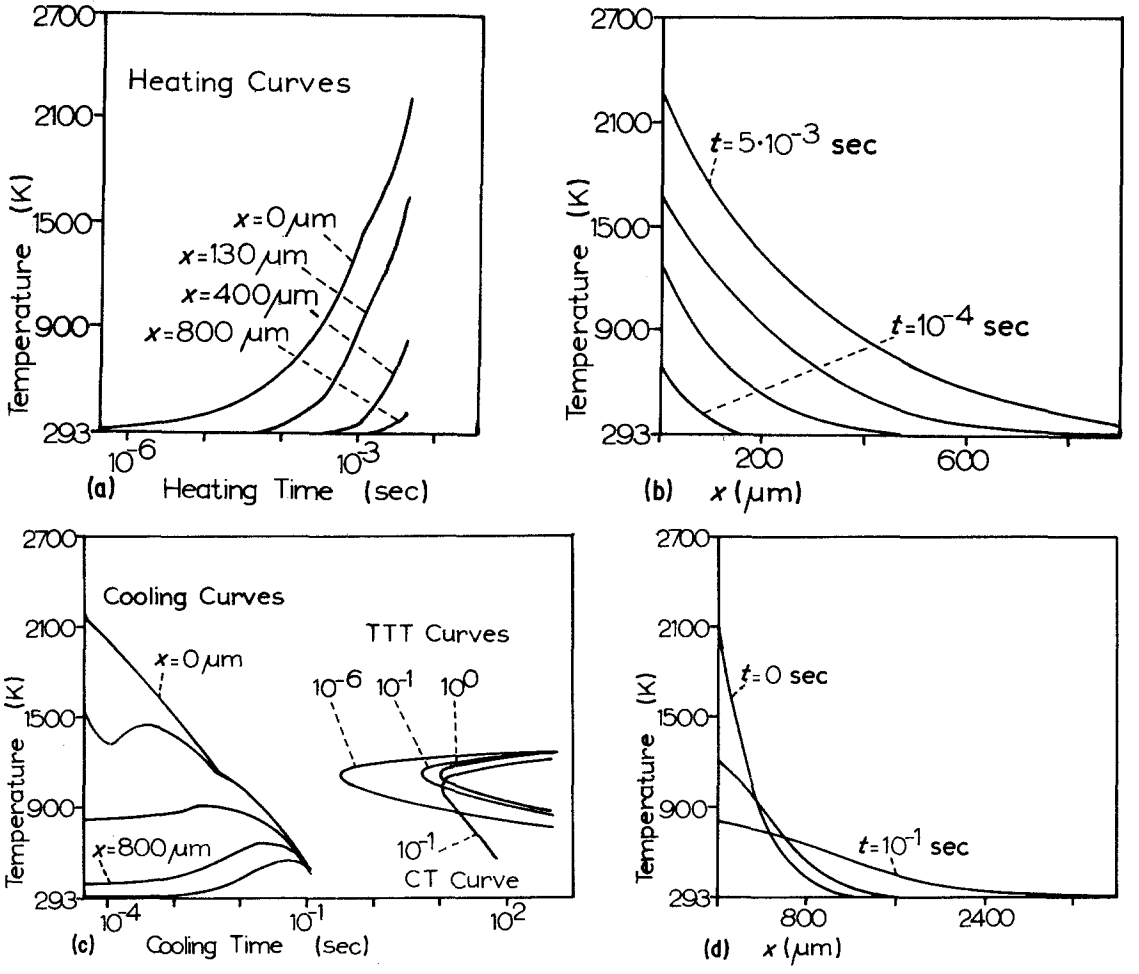

Figure 4 Melting and solidification, calculated for electron beam glazing of $Nb_{40}Ni_{60}$. (The end of heating is zero time for cooling.) (a) Heating curves for different distances from the surface, (b) temperature profiles during heating, (c) solidification–cooling curves for different depths, TTT curves and CT curve and (d) temperature profiles during cooling.

this process together with TTT curves and CT curves. The input data are given in Table I. It can be seen that during contact the ribbons are quenched down to different temperatures, depending on their thickness. The 10 μm thick tape shows glassy solidification while tapes of the order of 20 μm thick may be partially crystalline. In tapes about 50 μm thick or more total crystallization is expected.

Fig. 3 shows the temperature profiles for the three tapes of different thickness. The fact that the temperature gradients are not pronounced indicates that for these thicknesses the heat transfer to the substrate and not the conduction within the tape is the dominating process. Since the heat transfer coefficient and the contact time were the same it is apparent that the different heat contents determine the solidification behaviour.

The predicted and experimentally observed results are in good agreement. To check the TTT curves more accurately, the metallic glass ribbons were annealed quasi-isothermally in a differential scanning calorimeter (heating rate 320 K min^{-1} from 293 K min^{-1} to $T_1 = 600$, 625, 650 and 675 K, thereafter heating at 1.25 K min^{-1} until completion of crystallization). In the time range accessible to experiment (2 to 100 min) the program predicted the observed temperatures within experimental accuracy. It is difficult to predict the course of crystallization because metastable or supersaturated phases can arise, the thermodynamic properties of which are not known. This is discussed elsewhere [15].

4.2. Electron beam melting

Electron beam melting was used to produce a Ni–Nb metallic glass layer on a Nb single crystal. The surface alloy was obtained by spraying Ni onto

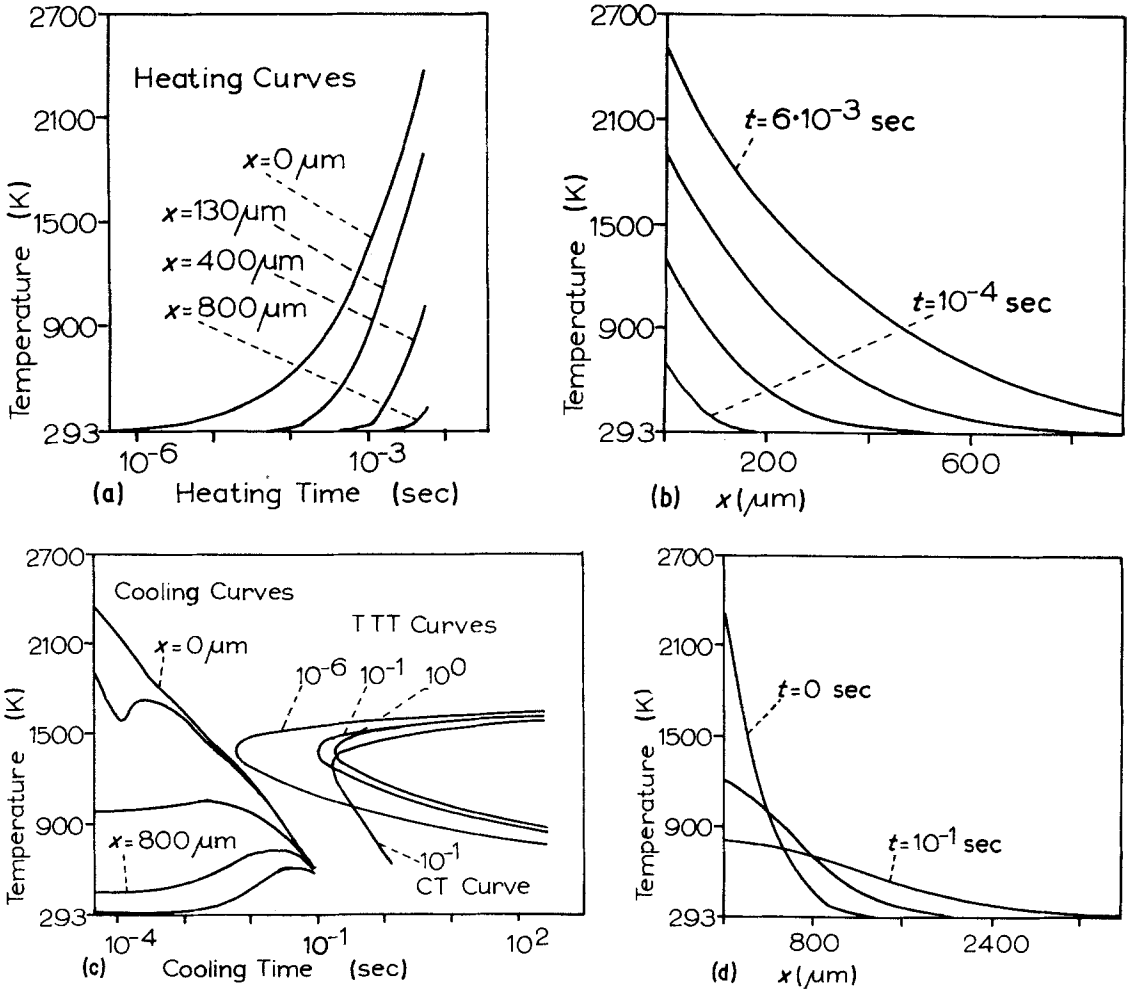

Figure 5 Melting and solidification, calculated for electron beam glazing of $Nb_{70}Ni_{30}$. (a) Heating curves for different distances from the surface, (b) temperature profiles during heating, (c) solidification–cooling curves for different depths, TTT curves and CT curve and (d) temperature profiles during cooling.

the surface. Test runs were necessary to establish the focussing conditions and the efficiency of the beam. A glass layer of 40 to 60 μm thickness was produced. Between the glassy layer and the substrate a 2 to 5 μm thick dendritic zone could be observed. The predicted results for $Nb_{40}Ni_{60}$ and $Nb_{70}Ni_{30}$ are shown in Figs 4 and 5 respectively. The electron microscope studies showed that up to molten layers of 20 to 80 μm the predicted amorphous state was indeed observed [16, 17]. The experimental verification of the solidification of surface alloyed and subsequently laser or electron beam treated surface layers is much more difficult than for melt-spun ribbons for the following reasons:

(a) The concentration of the melt is determined by the depth of the molten layer chosen as well as the thickness and composition of the deposited layer.

(b) Up to the present time, phase separation has not been taken into account in the theoretical work.

(c) A concentration gradient exists in the boundary layer with the substrate.

A comparison of Fig. 4 with 5 shows the effect, for otherwise identical experimental conditions, of a change in concentration from $Nb_{40}Ni_{60}$ to $Nb_{70}Ni_{30}$. Fig. 6 shows three typical experimentally determined profiles:

(a) Complete crystallization on an epitaxial boundary layer was observed for concentrations too far removed from the glass-forming concentration, as shown in Fig. 6a.

(b) When phase separation takes place (Fig. 6b),

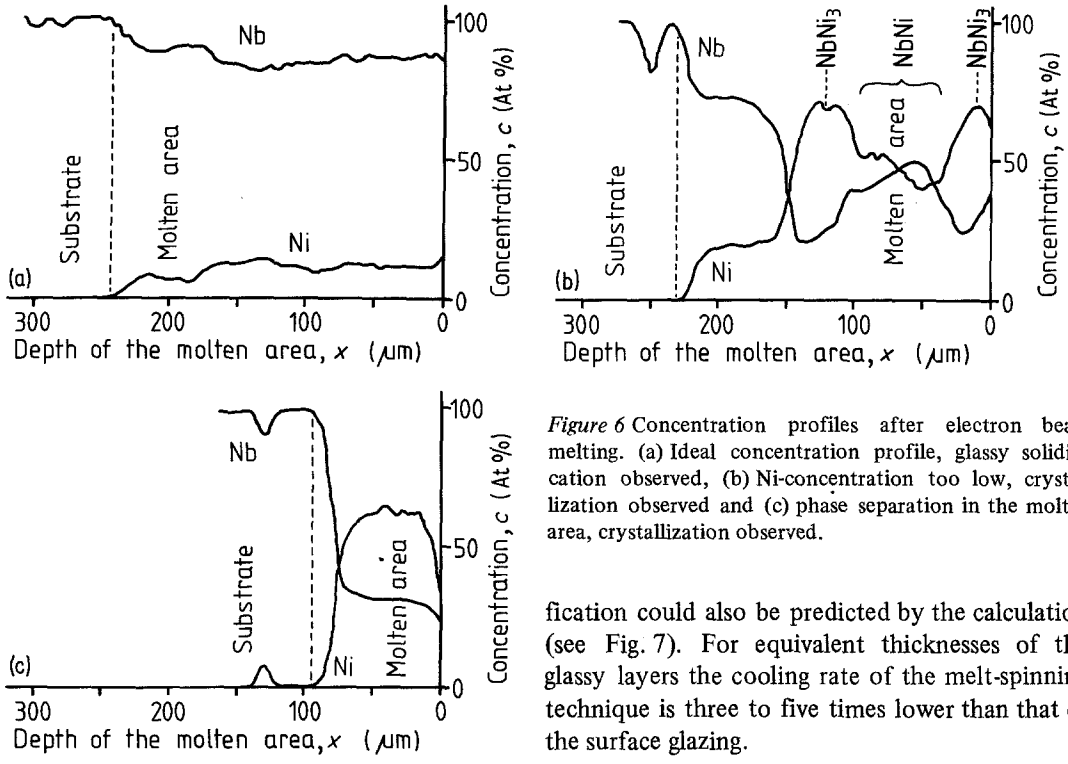

Figure 6 Concentration profiles after electron beam melting. (a) Ideal concentration profile, glassy solidification observed, (b) Ni-concentration too low, crystallization observed and (c) phase separation in the molten area, crystallization observed.

two different glassy or crystalline structures can develop [18].

(c) This is the only result which can be compared directly with predicted results. Here a suitable concentration $\sim Nb_{40}Ni_{60}$ for glass-forming was achieved over a large depth of the molten layer (Fig. 6c). Nevertheless a 5 to 10 μm thick region is observed in which the glass concentration (used in the calculation) changes to that of the substrate (pure Nb). Thus it is not surprising that for heterogeneously nucleated layers a dendritic layer is observed as predicted when the growth rate is the rate controlling factor, (Uhlmann [12]).

For comparison of the melt-spinning and the electron beam glazing results, $Nb_{40}Ni_{60}$ metallic glass tapes of 50 μm were produced and investigated. The experimentally found amorphous solidification could also be predicted by the calculation (see Fig. 7). For equivalent thicknesses of the glassy layers the cooling rate of the melt-spinning technique is three to five times lower than that of the surface glazing.

4.3. Laser glazing

In a third series of experiments a layer of boron was plasma-sprayed onto the surface of a Cr-steel [19]. The focussing and reflection conditions were established in test runs. The heating and cooling curves were then calculated for different experimental parameters (e.g. Fig. 8). A glassy layer was predicted for a melted depth of 10 to 40 μm (Fig. 6a). Electron micrographs confirm this prediction [17, 19]. The dendritic transition zone to the matrix has a thickness of 5 to 10 μm which is of the same order of magnitude as the calculated value (1 μm) considering the above mentioned influence of the concentration profile. Deeper melting (*ca* 500 μm) resulted in a completely crystallized layer as was correctly predicted.

It should be emphasized that a computer

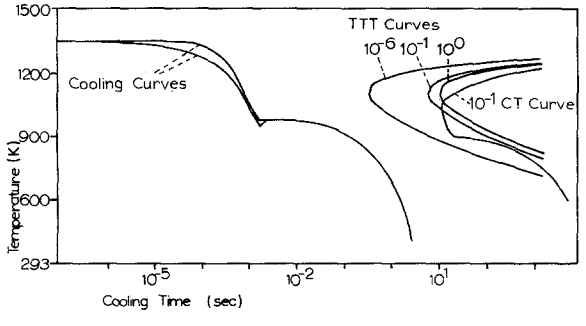

Figure 7 Calculated solidification during melt-spinning of $Nb_{40}Ni_{60}$ tapes. Upper and lower cooling curves correspond to the top-side and contact-side of the tape.

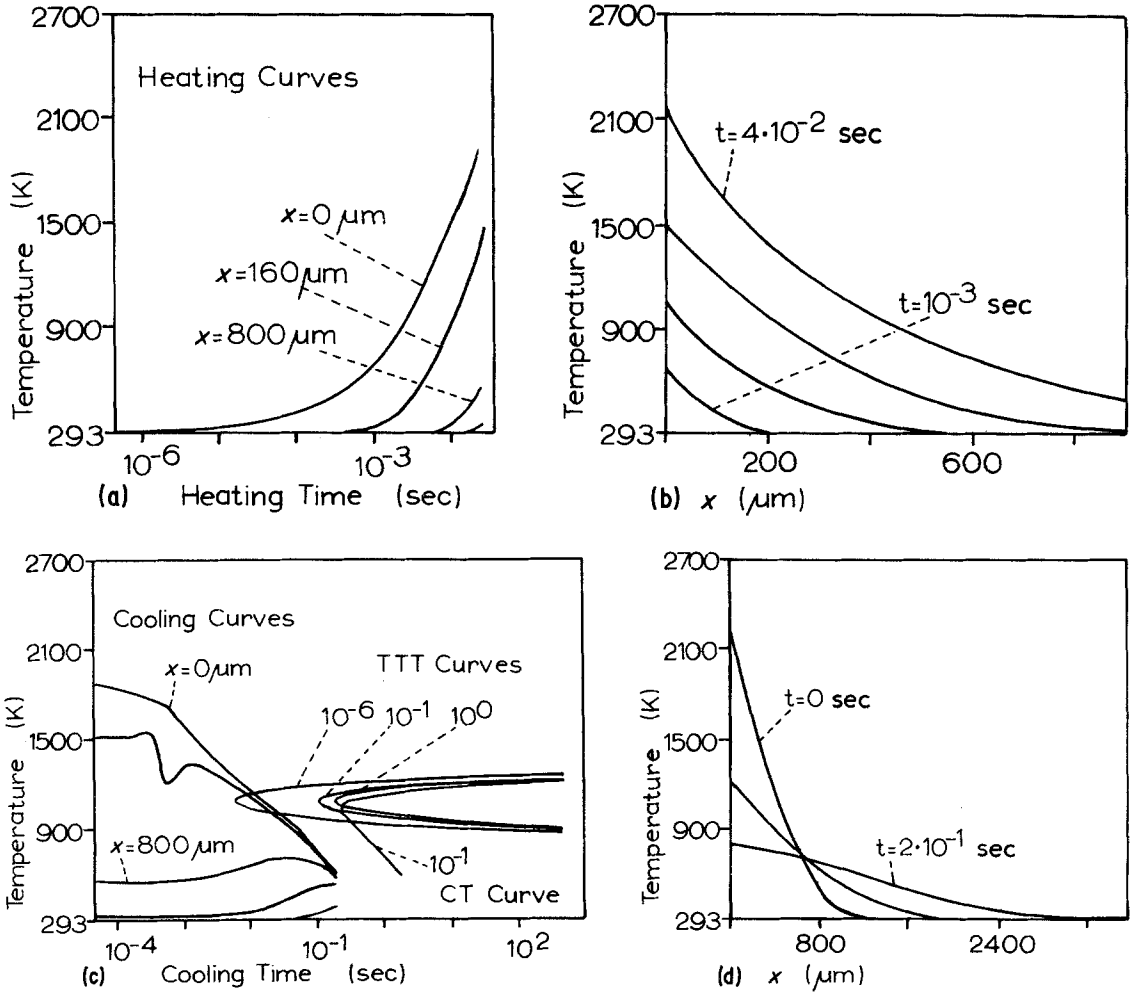

Figure 8 Melting and solidification, calculated for laser glazing of $(Fe_{87}Cr_{13})_{83}B_{17}$. (a) Heating curves for different distances from the surface, (b) temperature profiles during heating, (c) solidification–cooling curves for different depths, TTT curves and CT curve and (d) temperature profiles during cooling.

program like this can only describe the experimental results when certain assumptions are made. Nevertheless valuable support is obtained in formulating the experimental procedure. It is assumed that during heating a complete mixture of the components takes place and that during subsequent cooling no phase separation occurs. This is a necessary assumption if glassy solidification is studied. If the crystallization itself is to be described there are other simplifications necessary, see e.g. Tacke *et al.* [20]. This will be published shortly [21]. The program is available on request.

Acknowledgements

The work was supported by the SFB 126 Clausthal/Göttingen (German Science Foundation). The authors thank B. L. Mordike for helpful discussions and assistance in the preparation of the manuscript.

References

1. P. DUWEZ, R. H. WILLENS and W. KLEMENT, *J. Appl. Phys.* **31** (1960) 1136.
2. H. A. DAVIES, *Rev. Chim. Min.* **16** (1969) 349.
3. J. J. GILMAN and H. J. LEAMY, "Metallic Glasses" (American Society of Metals, Ohio, 1979).
4. R. W. K. HONEYCOMBE, 3rd International Conference on Rapidly Quenched Metals, Sussex, Brighton, 1978, Vol. 1 (Metals Society, London, 1978) p. 73.
5. H. HILLMANN and H. R. HILZINGER, *ibid.* Vol. 1, p. 22.
6. H. A. DAVIES, *ibid.* Vol. 1, p. 1.
7. W. A. GRANT, A. ALI, L. T. CHADDERTON, P. J. GRUNDY and E. JOHNSON, *ibid.* Vol. 1, p. 63.
8. R. C. RUHL, *Mater. Sci. Eng.* **1** (1967) 313.
9. T. R. ANTHONY and H. E. CLINE, *J. Appl. Phys.* **48** (1977) 3888.

10. H. E. CLINE and T. R. ANTHONY, *ibid.* **48** (1977) 3895.
11. H. A. DAVIES, *Phys. Chem. Glasses* **17** (1976) 159.
12. D. R. UHLMANN, "Materials Science Research", Vol. 4 (Plenum Press, New York, 1969) pp. 172–97.
13. R. A. GRANGE and J. M. KIEFER, *Trans. ASM* **29** (1941) 85.
14. E. SCHMIDT, "Einführung in die technische Thermodynamik" (Springer-Verlag, Berlin, 1963).
15. G. HUNGER, H. -W. BERGMANN and H. U. FRITSCH, Conference on Metallic Glasses: Science and Technology, 1980, Budapest.
16. H. -W. BERGMANN and B. L. MORDIKE, Conference on Metallic Glasses: Science and Technology, 1980, Budapest.
17. *Idem, J. Mater, Sci.* **16** (1981) 863.
18. G. CIERNIOCH, H. -W. BERGMANN and B. L. MORDIKE, to be published.
19. H. -W. BERGMANN and B. L. MORDIKE, *Z. Metallkde.* **71** (1980) 658.
20. K. -H. TACKE, A. GRILL, KEN-ICHI MIYAZAWA and K. SCHWERDTFEGER, Mitteilungen aus dem MPI für Eisenforschung, (Max Planck Institute, 1980).
21. H. -W. BERGMANN and H. U. FRITSCH, International Conference on Metallic Glasses, Japan, 1981.

Received 22 September 1980 and accepted 8 January 1981.